Definition of a New Circular Space-Filling Curve

$\beta\Omega$-Indexing

Jens-Michael Wierum

Paderborn Center for Parallel Computing, PC^2
Fürstenallee 11, 33102 Paderborn, Germany
jmwie@upb.de
http://www.upb.de/pc2/

PADERBORN
CENTER FOR
PARALLEL
COMPUTING

Technical Report PC^2
TR-001-02
March 2002

Abstract. This technical report presents the definition of a circular Hilbert-like space-filling curve. Preliminary evaluations in a simulation environment have shown good locality preserving properties. The results are compared with known bounds for other indexing schemes: Hilbert-, Lebesgue-, and H-Indexing. We evaluated partitions induced by the indexing schemes and uses the diameter and the surface as measures. For both we present worst case and average case results.

1 Introduction

Space-filling curves are geometric representations of bijective mappings $M : \{1, \ldots, N^m\} \to \{1, \ldots, N\}^m$. The curve M traverses all N^m cells in the m-dimensional grid of size N. An (historic) overview on space-filling curves is given in [11].

In computational geometry data structures based on space-filling curves are often used for requests on axis aligned bodies of arbitrary size. The aim of the requests is to find all points located in such multidimensional intervals. Those types of requests are needed in many applications like N-body simulations [12], image compression and browsing [10, 4], databases [2], and contact search in finite element analysis [5]. An overview on this and other techniques for range searching in computational geometry is given in [1]. Space-filling curves have other locality properties which are e. g. useful in parallel finite element simulations [3, 7].

Due to the varying requirements on the *locality* properties, different metrics have been used to qualify, compare, and improve space-filling curves. Here we use two metrics to examine the locality properties of the new curve: *diameter* and *surface* of an induced partition. We compare the hypothetical bounds with known analytical bounds of other space-filling curves: Hilbert-, Lebesgue-, and H-indexing. Descriptions of the generation of those curves can be found in [11, 9].

The next section introduces the $\beta\Omega$-indexing. Section 3 defines the metrics used in this report. The following section briefly describes the implemented simulation environment. Afterwards, the evaluated locality values are presented and discussed.

2 The $\beta\Omega$-Indexing

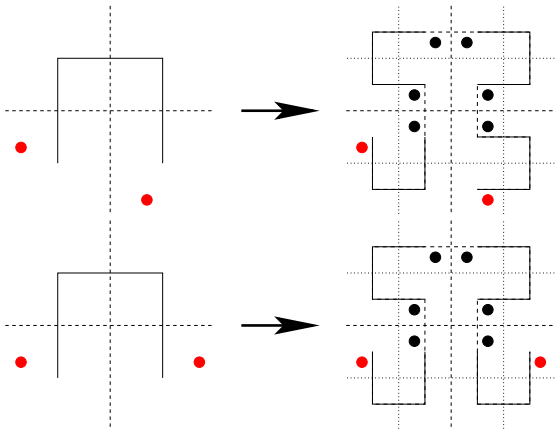

Fig. 1. Recursive definition of the $\beta\Omega$-indexing.

The $\beta\Omega$-indexing uses the same U-like base geometry as the Hilbert curve. We define two sub types of this base geometry with two different refinement rules. The sub types illustrated in Figure 1 are labeled with small dots. They represent the two end points of the curve within this quarter. The upper sub curve interconnects end points on neighbored borders of the quad while the lower curve interconnects end points on opposite borders of the quad. In the following we will denote them as *bended* and *straight* sub curves. A bended object is split into three bended and one straight quarters. A straight object is split into four bended quarters.

Fig. 2. Explanation for the name of the curve.

The name $\beta\Omega$-indexing is derived from the way the curve passes a quad of size 4×4. Figure 2 shows the the curves for the two sub types in a smoother way.

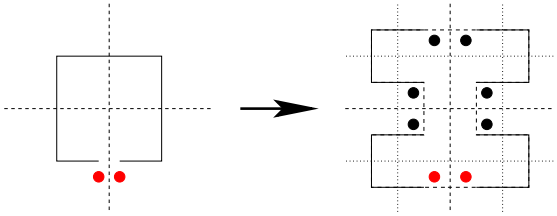

Fig. 3. Special rule for the first refinement step.

It is obvious that any sub type chosen at the highest level gives asymptotic comparable locality properties. To get a circular curve we need a special rule shown in Figure 3. The initial area is split into four bended objects.

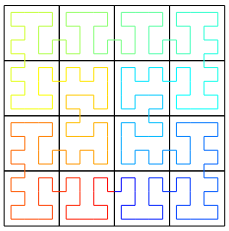

Fig. 4. Curve for a grid of size 16×16 (4 refinement steps).

Figure 4 shows the curve for a grid of size 16×16. In the appendix curves for larger grids are plotted (see Figures 7, 8, and 9).

2.1 Observations

During the refinement, the relative position of the end points are lying alternating on the left and the right hand side of the new separator. E. g. in the bended rule of Figure 1 one end point lies on the right hand side of the vertical separator. In the next refinement step it lies on the left hand side of the new vertical separator of the lower right quarter. In the next refinement step it will be on the right hand side, and so on. It follows, that the junction of the curve between two quarters converges to one-third or two-thirds of their common border.

As mentioned above, the bended sub curves are split into three bended and a single straight while the straight one is split into four bended objects. It follows that roughly $4/5$ of the objects are of bended type while $1/5$ is straight. The exact value depends on the examined level l of refinement: In the even case we have $\frac{4 \cdot (4^l - 1)}{5}$ bended objects and in the odd case $\frac{4 \cdot (4^l + 1)}{5}$. It follows, that we have $\frac{4^i + 4}{5}$ or $\frac{4^i - 4}{5}$ straight objects. This fact can be easily proven by an complete induction.

3 Locality Metrics

The *diameter* metrics describes the ratio of index interval to maximum distance within the partition induced by this index-range. Analytical results are published for different indexing schemes like Hilbert curve and H-indexing for Manhattan metric, Euclidean metric, and maximum metric in worst case [6, 9]. We use an modification of the measure defined by Gotsman and Lindenbaum [6]:

Definition 1 (locality). *Let* curve *be an indexing scheme, p an index range, $V(p) = |p|$ the size (volume) of the partition, and $d(p)$ the maximal Euclidean distance (diameter) within it. $L^{curve}(p)$ defines the* locality *of the partition given by index range p:*

$$L^{curve}(p) = \frac{d^{curve}(p)^2}{V(p)} \tag{1}$$

This formulation can be extended to a locality *measure of an indexing scheme:*

$$L^{curve}_{\max} = \max_p\{L^{curve}(p)\} \tag{2}$$

$$L^{curve}_{\text{avg}} = \text{avg}_p\{L^{curve}(p)\} \tag{3}$$

Gotsman and Lindenbaum concentrate on the worst case scenarios. They based their definition on the distance of two indices of the curve rather than on the partition induced by those indices. It is obvious that both definitions result in the same locality value for the maximum operation. For us the modified definition seems to be a more meaningful approach in the average case, because we are more interested in the structure of induced partitions.

The *surface* metrics examines the boundary of a partition which is induced by an interval of a space-filling curve. This property is necessary for the partitioning in parallel programming, e. g. in finite element analysis. Experimental results of this relationship for uniform grids and unstructured meshes can be found in [14]. Analytical evaluations for Hilbert and Lebesgue curve are given in [8]. The *quality coefficient* represents a normalized value for the quality of the induced partition in an uniform grid of size $n \times n$. We use the shape of an optimal partition, i. e. the square, as a reference:

Definition 2 (quality coefficient). *Let* curve *be an indexing scheme, p an index range, $S(p)$ the surface of a partition, and $V(p) = |p|$ the size (volume) of it. $C^{curve}(p)$ defines the* quality coefficient *of the partition given by index range p:*

$$C^{curve}(p) = \frac{S^{curve}(p)}{4 \cdot \sqrt{V(p)}} \tag{4}$$

This formulation can be extended to a quality coefficient *of an indexing scheme:*

$$C^{curve}_{\max} = \max_p\{C^{curve}(p)\} \tag{5}$$

$$C^{curve}_{\text{avg}} = \text{avg}_p\{C^{curve}(p)\} \tag{6}$$

4 Simulation Environment

We have developed a simulation environment for the evaluation of the locality of space-filling curves. The data structures allow the examination of unstructured meshes of arbitrary dimension. Each element (cell) has informations about its geometric position and pointers to its adjacent cells. Based on the geometric information of the cells any space-filling curve can be created by generating the corresponding index-permutation. All index-intervals of a predefined size are examined to find the worst case scenario and the average case quality.

4.1 Surface

The examination of the induced surface for an interval of size V is quite easy. We need two functions for the control of the surface size, one for adding and one for deleting a cell of the partition. In both cases we have to check all neighbors of the added/deleted cell for being inside or outside the actual partition to adjust the surface size. In the start-up phase the cells $0, \ldots, V-1$ are added to the partition. For each following partition a new element is appended while the first is deleted. Note, that without any overhead the surface quality for $V+1$ can be computed in the same run.

4.2 Diameter

The calculation of the partitions diameter is more expensive. A brute force approach needs $O(V^2)$ distance calculations for a V-cell partition. On the other hand, any restriction of the search-space (e. g. examine only cells on the border of the partition) is more sophisticated and it depends on the characteristic of the space-filling curve whether it pays off.

In our examinations we are interested in the dependency on the locality metrics for increasing partition sizes. That means we want to know all values for partitions of sizes $1, \ldots, V$. We can increase the overall efficiency of the simulation run, if we calculate all diameters for partitions of size $1, \ldots, V$ with a fixed first cell. In each step we add a single cell. The diameter of the increased partition is the maximum of the old diameter and the largest distance of all old cells to the new one. Again, it is possible to restrict the distance calculations on the border cells of the partition.

5 Induced Diameter

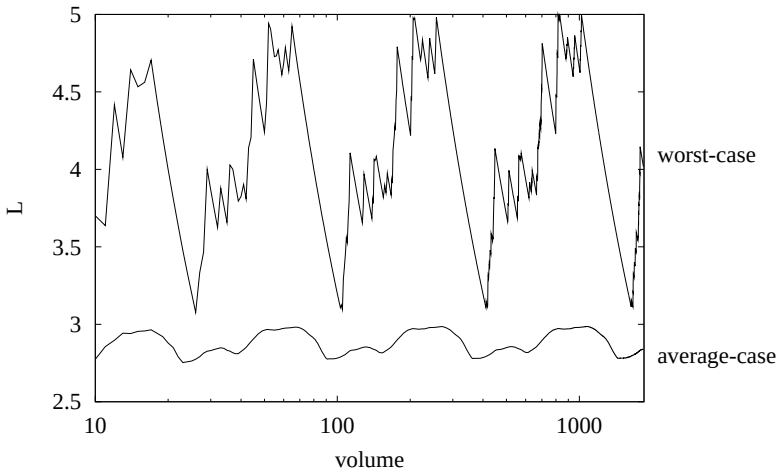

Fig. 5. Induced diameter L of different partitions in the grid.

In Figure 5 the relative diameter of a partition induced by the $\beta\Omega$-indexing is presented for the average and worst case. A partition of size *volume* in a grid of size 512×512 is evaluated. The value is normalized to the size of the partition: $L = \frac{d^2}{volume}$, as proposed by Gotsman and Lindenbaum [6].

We can find hypothetical bounds of 3 for the average case and 5 for the worst case. In worst case, bounds for Hilbert- and H-indexing are known [9]:

$$d^{\mathrm{Hilbert}}(i,j) \leq \sqrt{6.01 \cdot |i-j|} \tag{7}$$

$$d^{\mathrm{H-indexing}}(i,j) \leq \sqrt{4 \cdot |i-j|} + \sqrt{10} \ , \tag{8}$$

with i, j as curve indices and $volume = |i-j|$.

The locality of the $\beta\Omega$-indexing lies between those two indexing schemes. Following the proof for $L_{\max}^{\mathrm{Hilbert}} \leq 6\frac{2}{3}$ in [6], it is possible to show $L_{\max}^{\beta\Omega-\mathrm{indexing}} \leq 5\frac{2}{3}$. That means, we can proof that the $\beta\Omega$-indexing is of higher locality than the Hilbert-indexing. The proof for the sharper bound in [9] (Eq. 7) does not seem to be appropriate for the $\beta\Omega$-indexing because of the different refinement rules for the two sub types.

6 Induced Surface

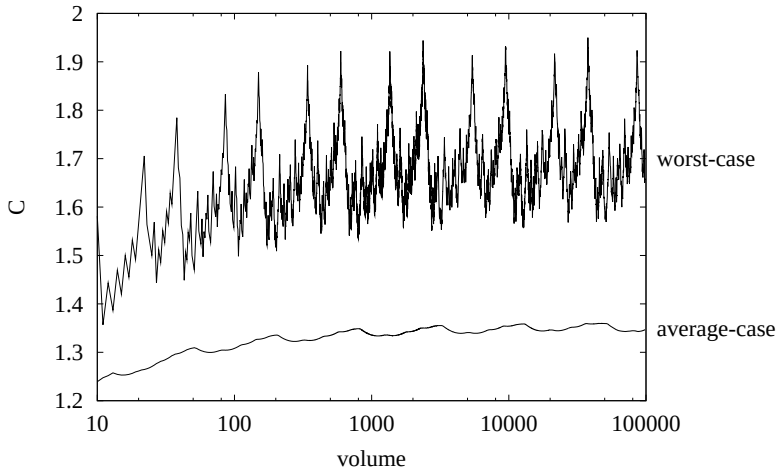

Fig. 6. Normalized induced surface C of different partitions in the grid.

In Figure 6 the surface quality of a partition induced by the $\beta\Omega$-indexing is presented. A partition of size *volume* in a grid of size 1024×1024 is evaluated. The value is normalized to the surface size of an optimal partition: $C = \frac{S}{4 \cdot \sqrt{volume}}$, as proposed by Zumbusch [14].

Hypothetical bounds are 1.95 for the worst case and 1.37 for the average case. Known bounds are:

$$1.8605 < 3 \cdot \sqrt{\frac{5}{13}} \leq C_{\max}^{\text{Hilbert}} \tag{9}$$

$$1.8371 < 3 \cdot \sqrt{\frac{3}{8}} - \varepsilon \leq C_{\max}^{\text{Lebesgue}} \leq \frac{96}{\sqrt{2730}} < 1.8374 \tag{10}$$

for the worst-case and

$$C_{\text{avg}}^{\text{Lebesgue}} \leq \frac{5}{2 \cdot \sqrt{3}} < 1.4434 \tag{11}$$

for the average-case [8, 13].

The evaluations show that the $\beta\Omega$-indexing is worse in maximum analysis compared to the Hilbert- and Lebesgue-indexing. On the other hand, the average case result is better than those for the Lebesgue-indexing. Furthermore, $\beta\Omega$-indexing seems to have a surface quality which is even better than that of Hilbert-indexing (cf. [8]).

7 Conclusion

The introduced $\beta\Omega$-indexing is a circular space-filling curve. Preliminary evaluations of the locality properties show that it has moderate quality for the two presented measures. Future work will include an extensive simulative evaluation of other curves to get comparable hypothetical bounds. Furthermore, the evaluated bounds should also be confirmed by analytical results.

References

1. P. K. Agarwal and J. Erickson. Geometric range searching and its relatives. *Advances in Discrete and Computational Geometry*, 1998.
2. T. Asano, D. Ranjan, T. Roos, E. Welzl, and P. Widmayer. Space-filling curves and their use in the design of geometric data structures. *Theoretical Computer Science*, 181:3–15, 1997.
3. J. Behrens and J. Zimmermann. Parallelizing an unstructured grid generator with a space-filling curve approach. In A. Bode, T. Ludwig, W. Karl, and R. Wismüller, editors, *Euro-Par 2000*, number 1900 in LNCS, pages 815–823. Springer, 2000.
4. S. Craver, B.-L. Yeo, and M. Yeung. Multilinearization data structure for image browsing. In *SPIE – The International Society for Optical Engineering*, 1998.
5. R. Diekmann, J. Hungershöfer, M. Lux, L. Taenzer, and J.-M. Wierum. Using space filling curves for efficient contact searching. In *Proc. IMACS*, Lausanne, 2000.
6. C. Gotsman and M. Lindenbaum. On the metric properties of discrete space-filling curves. *IEEE Transactions on Image Processing*, 5(5):794–797, May 1996.
7. M. Griebel and G. Zumbusch. Parallel multigrid in an adaptive PDE solver based on hashing and space-filling curves. *Parallel Computing*, 25:827–843, 1999.
8. J. Hungershöfer and J.-M. Wierum. On the quality of partitions based on space-filling curves. In *Computational Geometry and Applications, CGA'02/ICCS'02*, LNCS. Springer, to appear in 2002.
9. R. Niedermeier, K. Reinhardt, and P. Sanders. Towards optimal locality in mesh-indexings. In B. S. Chlebus and L. Czaja, editors, *Fundamentals of Computation Theory*, number 1279 in LNCS, pages 364–375. Springer, 1997.
10. R. Pajarola and P. Widmayer. An image compression method for spatial search. *IEEE Transactions on Image Processing*, 9(3):357–365, 2000.
11. H. Sagan. *Space Filling Curves*. Springer, 1994.
12. S.-H. Teng. Provably good partitioning and load balancing algorithms for parallel adaptive N-body simulation. *SIAM Journal on Scientific Computing*, 19(2):635–656, 1998.
13. J.-M. Wierum. Average case quality of partitions induced by the Lebesgue indexing. Technical Report TR-002-01, Paderborn Center for Parallel Computing, http://www.upb.de/pc2/, 2001.
14. G. Zumbusch. On the quality of space-filling curve induced partitions. *Zeitschrift für Angewandte Mathematik und Mechanik*, 81, SUPP/1:25–28, 2001.

8 Appendix

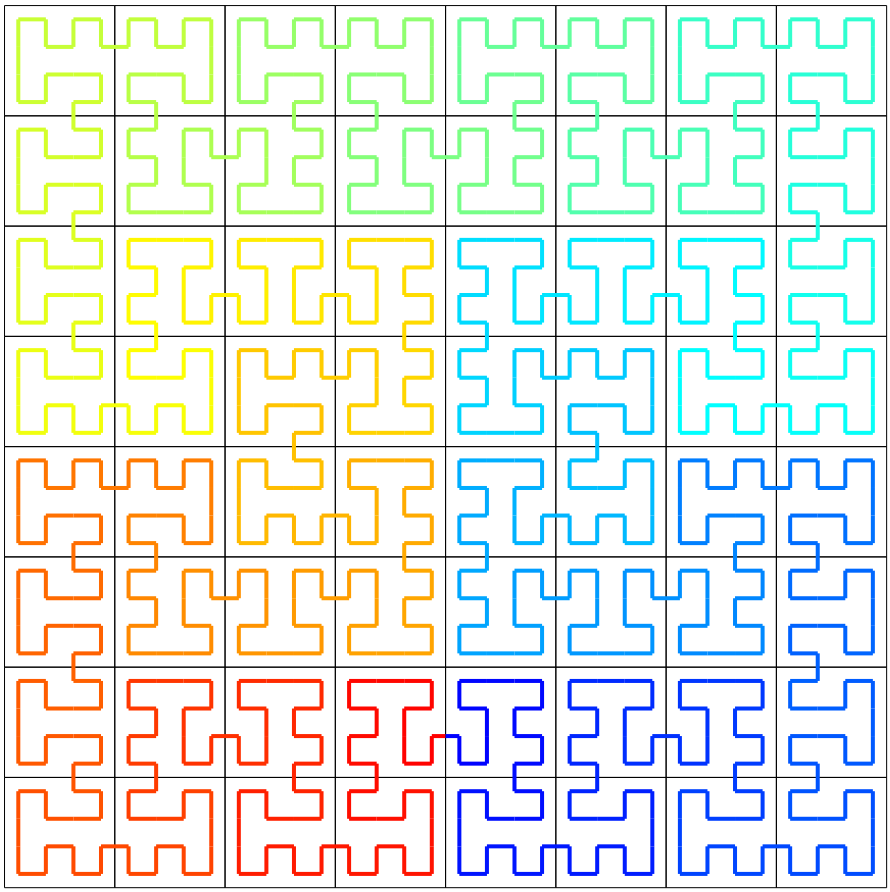

Fig. 7. Curve for a grid of size 32×32 (5 refinement steps).

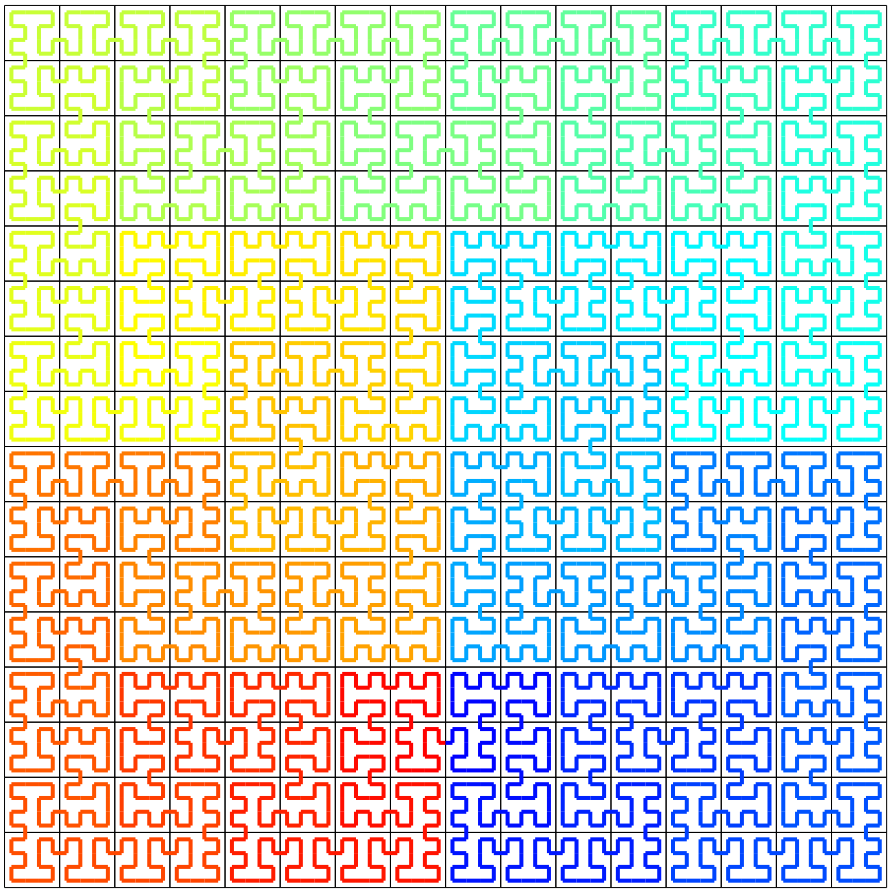

Fig. 8. Curve for a grid of size 64×64 (6 refinement steps).

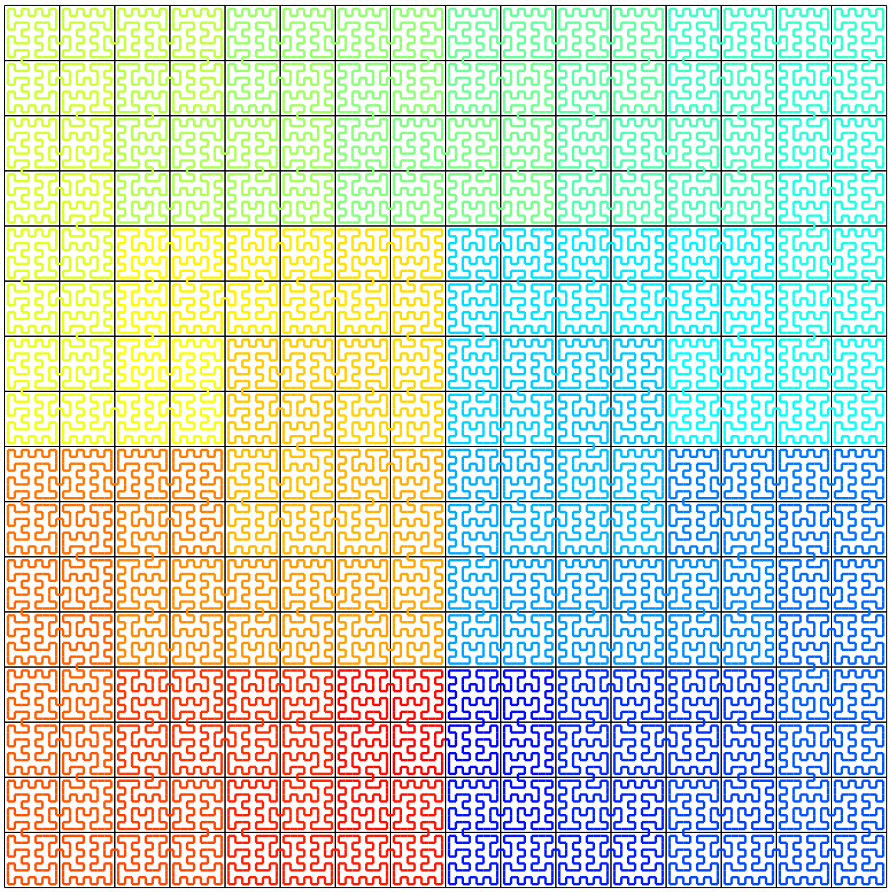

Fig. 9. Curve for a grid of size 128 × 128 (7 refinement steps).